AFCRL- 67-0450

Influence of Single Scattering Albedo on Reflected and Transmitted Light from Clouds

Authors

Gilbert N. Plass
George W. Kattawar

Southwest Center for Advanced Studies
Dallas, Texas

Contract No. AF19(628)-5039

Project No. 4076

Task No. 407604

Scientific Report No. 4

12 July 1967

This research was partially supported by the National Aeronautics and Space Administration

Contract Monitor
Robert W. Fenn
Optical Physics Laboratory

Prepared
for

AIR FORCE CAMBRIDGE RESEARCH LABORATORIES
OFFICE OF AEROSPACE RESEARCH
UNITED STATES AIR FORCE
BEDFORD, MASSACHUSETTS 01730

AFCRL- 67-0450

Influence of Single Scattering Albedo on Reflected and Transmitted Light from Clouds

Authors

Gilbert N. Plass
George W. Kattawar

Southwest Center for Advanced Studies
Dallas, Texas

Contract No. AF19(628)-5039

Project No. 4076

Task No. 407604

Scientific Report No. 4

12 July 1967

This research was partially supported by the National Aeronautics and Space Administration

Contract Monitor
Robert W. Fenn
Optical Physics Laboratory

Prepared
for

AIR FORCE CAMBRIDGE RESEARCH LABORATORIES
OFFICE OF AEROSPACE RESEARCH
UNITED STATES AIR FORCE
BEDFORD, MASSACHUSETTS 01730

Influence of Single Scattering Albedo on Reflected and Transmitted Light from Clouds

GILBERT N. PLASS and GEORGE W. KATTAWAR

Abstract

The dependence of the reflected and transmitted light from clouds on the single scattering albedo ω_o is studied. The multiply scattered path of the photon in the cloud is accurately simulated by Monte Carlo techniques. When the cloud is thin and the surface albedo A = 0, the reflected and transmitted radiances vary nearly as ω_o for fixed angles of incidence and observation and they depend strongly on the value of A. As ω_o becomes small and for thick clouds, the reflected radiance approaches more closely the value calculated from the single scattering phase function. As the absorption increases the transmitted radiance at the zenith becomes larger relative to the value near the horizon. Also as the optical thickness increases, the maximum of the transmitted radiance moves from the incident direction toward the zenith. The variations in the flux and the mean optical path are also discussed.

The authors are with the Southwest Center for Advanced Studies, Dallas, Texas 75230.

Introduction

The reflected and transmitted radiance from clouds depends on a number of parameters. Some of the important factors include the number and size distribution of the water droplets, the wavelength of the light, the single scattering albedo, the albedo of the planetary surface, the angle of the incoming solar radiation, and the optical thickness of the cloud together with its shape. In order to understand the complex phenomenon of multiple scattering from clouds it is important to study the influence of variations in just one of these parameters at a time while assuming realistic values for the remainder.

This paper is concerned only with variations in the single scattering photons. At wavelengths in the visible water is so weakly absorbing that it can be neglected for all practical purposes for the water amounts which occur in clouds. However, water has a number of strong absorption bands beginning in the near infrared. Some of these are so strong that more than half the incident radiation is absorbed by a single water droplet of the typical size which occurs in clouds.

The reflected and transmitted radiance is calculated as a function of the albedo for single scattering by a Monte Carlo method. This computer program has already been described in detail in the literature[1]. Briefly it calculates the radiance and flux at a number of detectors placed throughout the cloud for various surface albedos. A single scattering phase function is obtained from the Mie theory by integration over the particle size distribution. The probability of scattering

at any angle is accurately calculated including the sharp and strong forward peak of the distribution. Thus the calculation simulates accurately the numerous small angle scattering collisions which occur.

Although there are necessarily fluctuations in any Monte Carlo result, these can be reduced to acceptable levels when a sufficient number of photons are used. The Monte Carlo method appears to offer the only practical way to obtain data for a wide range of conditions including strong forward scattering, inhomogenities in the atmosphere, and the occurrence of several different processes which absorb and scatter the photon.

Fritz[2,3] and Twomey et al[4] have calculated the effects of light scattering from clouds by other methods and obtained very interesting results. The Monte Carlo method has been discussed by Hammersley and Handscomb[5] and has been applied to atmospheric problems by Collins and Wells[6]. However, all of these authors have considered only the case of pure scattering and have not included any absorption by the water droplets.

Cloud Model

The size distribution for the water droplets in a cumulous cloud chosen for this calculation is

$$n(r) = 2.373\ r^6\ \exp(-1.5r) \quad , \qquad (1)$$

where the radius r is expressed in microns and the concentration n is expressed in $cm^{-3}\ \mu^{-1}$. This is the distribution function used by Deirmendjian[7]. The single scattering phase function was calculated from the Mie theory by averaging over this distribution[1]. A wavelength of 0.7μ for the incident light and a real index of refraction of 1.33 for the water droplets was assumed for this calculation. This particular single scattering phase function was used for all of the calculations in this paper as we wished to study the effect of variations in the single scattering albedo alone. A more realistic calculation would have changed both the wavelength and index of refraction to agree with the assumed single scattering albedo. However, the changes would then have been due to two causes which could not be separated. Furthermore, separate calculations showed that changes in the radiance due to variations in the single scattering phase function are considerably smaller and often negligible compared to those due to changes in the single scattering albedo.

The single scattering phase function was calculated at 0.25° intervals in the forward direction near the strong forward scattering maximum and at 2° intervals in the backward direction where the functions undergoes several oscillations. The cumulative probability for scattering as a function of angle was obtained from interpolation between these calculated points. This large number of calculated points was found to be necessary in order to determine the single scattering phase function accurately. An integration of this quantity over the unit sphere was performed in order to check the accuracy of the volume

averaged phase function. This integral has the value of unity when there is no absorption. The results of the integration are always within a few hundredths of one percent of unity.

All calculations reported here assume reflection from a Lambert's surface as representative of the planetary surface. Results are reported for a surface albedo A of 0 and 1. The albedo for single scattering ω_o is varied in order to determine the influence of strong absorption on the radiance. The optical thickness τ of the cloud is defined in terms of the total cross section including the contributions from both scattering and absorption.

Reflected Radiance

The calculated reflected radiance from thin clouds ($\tau \blacksquare 0.1$) is shown in Figs. 1-3 for various values of the cosine of the polar angle of the incident beam (μ_o = -1.0, -0.5, -0.1). When the incident beam is in the vertical direction (μ_o = -1.0), the reflected radiance for A = 0 follows closely the value calculated from single scattering except near the horizon[1]. The reflected radiance for a particle value of the cosine of the scattering angle μ varies directly as ω_o, since the number of effective scattering centers in a particular direction of observation is also proportional to ω_o. This decrease in the reflected radiance in proportion to ω_o is accurately valid for $\mu > 0.6$ (μ is the cosine of the angle of reflected beam) and is approximately true for smaller values of μ. The actual values are smaller than those predicted from this relationship for angles near the horizon. This is because

the photon has an increased probability of being absorbed before it escapes from the cloud.

The reflected radiances for $\tau = 0.1$ and $A = 0$ are shown in Figs. 2 and 3 for $\mu_o = 0.5$ and -0.1 respectively. The curves for different values of ω_o are very similar. The radiance decreases approximately as ω_o with a slightly greater decrease near the horizon.

The reflected radiance for a thin cloud depends critically upon the surface albedo as is shown in Fig. 1. When $A = 1$ the reflected radiance which now includes the radiation reflected from the ground is nearly constant with angle. It decreases slightly as ω_o decreases, especially near the horizon. The results for $\mu_o = -0.5$ and -0.1 and $A = 1$ (not shown here) indicate that these variations become larger as the incident beam approaches the horizon. When $\mu_o = -0.5$ the reflected radiance for $\omega_o = 0.1$ is only 22% of its value for $\omega_o = 1$ when μ is near the horizon (the corresponding figure is 6.7% when μ_o ◘ -0.1). The differences are less near the zenith. For μ_o ◘ -0.1 and $\omega_o = 0.1$ the reflected radiance is 0.0135 on the near horizon, then nearly constant at 0.0115 until it starts decreasing at the far horizon to a value of 0.00381.

The reflected radiance for a cloud of intermediate thickness is shown in Fig. 4 ($\tau = 1.0$, $\mu_o = -1.0$). The curves for $A = 0$ are higher than those shown in Fig. 1 for $\tau = 0.1$. There is appreciable multiple scattering for τ ◘ 1. Thus the reflected radiance decreases by more than a factor ω_o as ω_o decreases, since the number of photons is reduced

by the factor ω_o at each collision. For the smaller values of ω_o the reflected radiance is largest near the zenith. The photons can escape near the zenith while undergoing few collisions because of the maxima in the single scattering phase function in the backward direction. With significant absorption only the photons that make a relatively small number of collisions contribute appreciably to the radiance. When A = 1 there is a pronounced decrease in the radiance away from the zenith. This is because very little radiation reflected from the surface can reach the top of the cloud at a small value of μ when the cloud is strongly absorbing.

The reflected radiance for a cloud of large thickness is shown in Fig. 5 (τ = 10, μ_o = -1.0). The magnitude of the radiance is appreciably higher when $\omega_o \geq 0.9$ for τ = 10 than for τ = 1 because of the large number of multiple scatterings undergone by a typical photon. This also smooths the curves so that there is less variation with μ. When there is appreciable absorption the radiance has a tendency to develop a more marked variation with μ with a maximum near the zenith. Especially for the ω_o = 0.1 curve, the lower values near the horizon are somewhat poorly defined due to a larger statistical error in the calculation of these smaller radiance values. The curves for surface albedo A = 1 are very similar to those for A = 0, since relatively little radiation can penetrate these thick clouds and be reflected back to the surface.

The reflected radiance for τ = 10 and μ_o = -0.5 and μ_o = -0.1 are shown in Figs. 6 and 7 respectively. As the absorption becomes stronger (ω_o becomes smaller), the reflected radiance approaches the curve

expected for single scattering from the phase function. This occurs even for thick clouds since only singly scattered photons can make an appreciable contribution to the intensity when ω_o is small. This effect is clearly visible in Figs. 6 and 7. For $\mu_o = -0.1$ and $\omega_o = 0.1$ the reflected radiance is 200 times smaller near the zenith than near the horizon.

Transmitted Radiance

The transmitted radiance for a thin cloud ($\tau = 0.1$) is shown in Figs. 8-10 for $\mu_o = -1.0$, -0.5, and -0.1. When absorption is present, the transmitted radiance for $\mu_o = -1.0$ is in most cases equal to ω_o multiplied by the transmitted radiance for $\omega_o = 1$. Near the horizon the computed value is somewhat less than would be predicted by this equation because of multiple scattering. For other angles of incidence the transmitted radiance decreases in general slightly more rapidly than is predicted from the ω_o rule. However, the general shape of the curves is remarkably constant as ω_o varies.

When $\mu_o = -0.5$ and -0.1 and $A = 1$, all the values for the transmitted radiance are increased over those for $A = 0$, particularly near the minima of the curves. However, the general shape of the curves remains the same.

The transmitted radiance for $\tau = 1$ and $\mu_o = -1.0$ is shown in Fig. 11. When $A = 0$ the radiance has a strong maximum around the zenith for all ω_o because of the numerous small angle scattering events which occur. The radiance decreases toward the horizon. This decrease is much more

rapid as the absorption increases. When A = 1 the radiance increases toward both the zenith and the horizon. The radiance near the horizon is increased significantly for all ω_o because of the backscattering from the reflected photons. Actually most of this radiance is contributed by photons that are reflected into a solid angle near the horizon and then are scattered through a relatively small angle into a downward direction.

The transmitted radiance for thick clouds (τ = 10) is shown in Figs. 12-14. For μ_o = -1.0 and A = 0 the radiance is always greater at the zenith than at the horizon. This difference greatly increases as the absorption increases until the zenith radiance is 260 times greater than the horizon radiance when ω_o = 0.1. When A = 1 the horizon radiance is increased significantly for all ω_o over the value for A = 0, whereas the zenith radiance is increased only for the cases where ω_o is near 1.

The shape of the transmitted radiance curves for the same ω_o values is very similar for μ_o = -0.5 and μ_o = -0.1. All information as to the direction of the original beam is essentially lost through the multiple collisions required to reach the bottom of the cloud. The maximum value for the radiance is always found near the zenith. The magnitude of the radiance values decreases as μ_o approaches the horizon since more of the photons are reflected out of the cloud after a few collisions by the forward maximum of the phase function. The expected increase in the statistical fluctuations of the result occurs when the radiance values are numerically small compared to unity.

Flux

The radiant flux which emerges from the cloud at its lower boundary when A = 0 is given in Table I for a number of different values of the parameters. When τ and μ_o are held fixed and the single scattering albedo ω_o is varied, the flux at the lower boundary always increases as ω_o increases. When τ = 0.1 or 1 the flux increases by an order of magnitude when ω_o increases from 0.1 to 1. However, the corresponding change for a thick cloud (τ ▫ 10 or 30) is many orders of magnitude. Obviously when there is appreciable absorption, very few photons can survive many collisions and penetrate a thick cloud.

Mean Optical Path

The mean optical path for both the reflected and transmitted photons is shown in Table I. When τ = 0.1, the mean optical path varies only slightly with ω_o since the majority of the photons undergo only a single scattering in this case.

When τ = 1 the mean optical path of the reflected photons decreases as ω_o decreases since the photons which can survive multiple collisions when there is considerable absorption stay nearer the upper surface on the average. Similarly the transmitted photons follow a shorter path on the average when the absorption is high. These effects are much more pronounced when τ ▫ 10 and 30. For example when τ = 30, the mean optical path for the reflected photons is 10.9 when ω_o = 0.1 and 59.9 for ω_o = 1. The transmitted mean optical path for this same cloud is 30.7 when ω_o = 0.1 and 81.9 when ω_o = 1. The value for ω_o = 0.1 is

quite remarkable since the cloud has an optical thickness of 30. Thus with this high absorption the only photons that can penetrate the cloud are those that pass through with only slight deviations from the original vertical direction. Obviously only a minute fraction of the photons can pass through a thick cloud in this manner as is shown by the very small value for the flux of 5.3×10^{-13}.

Table I.

Mean Optical Path and Flux at Lower Boundary for A = 0.

τ	μ_o	ω_o	Reflected mean optical path	Transmitted mean optical path	Flux at Lower Boundary
0.1	0.1	0.1	1.32	1.06	0.0322
0.1	0.1	0.5	1.35	1.06	0.184
0.1	0.1	1	1.34	1.04	0.452
0.1	0.5	0.1	0.808	0.270	0.0147
0.1	0.5	0.5	0.892	0.286	0.0768
0.1	0.5	1	0.850	0.286	0.163
0.1	1	0.1	0.320	0.113	0.00862
0.1	1	0.5	0.408	0.115	0.0440
0.1	1	0.9	0.441	0.116	0.0810
0.1	1	1	0.454	0.119	0.0905
1	1	0.1	2.68	1.13	0.0349
1	1	0.5	3.41	1.15	0.215
1	1	0.9	3.70	1.19	0.493
1	1	1	3.75	1.23	0.584
10	0.1	0.1	4.91	20.4	4.95×10^{-8}
10	0.1	0.5	8.86	20.4	4.04×10^{-5}
10	0.1	0.9	11.3	25.4	0.0254
10	0.1	1	12.9	28.0	0.201
10	0.5	0.1	8.43	17.7	6.50×10^{-6}
10	0.5	0.5	14.3	17.5	2.29×10^{-4}
10	0.5	0.9	18.4	22.7	0.0517
10	0.5	1	20.8	24.9	0.362
10	1	0.1	10.6	11.1	4.42×10^{-5}
10	1	0.5	15.5	11.5	2.48×10^{-3}
10	1	0.9	22.1	16.1	0.136
10	1	0.99	25.1	19.0	0.472
10	1	1	24.2	19.2	0.534
30	1	0.1	10.9	30.7	5.3×10^{-13}
30	1	0.5	17.4	31.8	4.51×10^{-9}
30	1	0.9	37.3	51.4	1.31×10^{-3}
30	1	0.99	55.7	76.3	0.113
30	1	1	59.9	81.9	0.227

References

1. G. N. Plass and G. W. Kattawar, J. Geoph. Res. (in press).

2. S. Fritz, J. Meteor. 11, 291 (1954).

3. S. Fritz, J. Opt. Soc. Amer. 10, 820 (1955).

4. S. Twomey, H. Jacobowitz, and H. B. Howell, J. Atm. Sci. 24, 70 (1967).

5. J. M. Hammersley and D. C. Handscomb, Monte Carlo Methods (John Wiley and Sons, Inc., New York, 1964).

6. D. G. Collins and M. B. Wells, Monte Carlo Codes for the Study of Light Transport in the Atmosphere, Vols. I and II, Radiation Research Associates, Inc., Fort Worth, Texas, 1965.

7. D. Diermendjian, Appl. Opt. 3, 187 (1964).

Legends for Figures

Fig. 1. Reflected radiance as a function of μ, the cosine of the zenith angle. The curves on the left and right portion of the figure are for A (surface albedo) = 0 and 1 respectively. The optical depth of the cloud τ = 0.1. The sunlight is incident vertically, μ_o (cosine of incident zenith angle) = -1.0. The single scattering albedo is ω_o. The incident intensity is normalized to unity.

Fig. 2. Reflected radiance for μ_o = -0.5, τ = 0.1, and A = 0 as a function of μ, the cosine of the zenith angle. The left hand portion of the graph refers to values averaged over the azimuthal angle for 90° on both sides of the original beam. The values on the right portion of the graph are for values averaged over the remaining azimuthal angles. Thus one intensity curve from left to right shows the variation from one horizon to the zenith and back to the other horizon averaged over the indicated azimuthal angles.

Fig. 3. Reflected radiance for μ_o = -0.1, τ = 0.1, and A = 0 as a function of μ. See caption for Fig. 2.

Fig. 4. Reflected radiance for μ_o = -1.0, τ = 1.0, and A = 0 and 1 as a function of μ. See caption for Fig. 1.

Fig. 5. Reflected radiance for μ_o = -1.0, τ = 10, and A = 0 and 1 as a function of μ. See caption for Fig. 1.

Fig. 6. Reflected radiance for μ_o = -0.5, τ = 10, and A = 0 as a function of μ. See caption for Fig. 2.

Fig. 7. Reflected radiance for $\mu_o = -0.1$, $\tau = 10$, and $A = 0$ as a function of μ. See caption for Fig. 2.

Fig. 8. Transmitted radiance for $\mu_o = -0.1$, $\tau = 0.1$, and $A = 0$ and 1 as a function of μ. The radiance from the unscattered photons of the original beam is not included. See caption for Fig. 1.

Fig. 9. Transmitted radiance for $\mu_o = -0.5$, $\tau = 0.1$, and $A = 0$ as a function of μ. See caption for Fig. 2.

Fig. 10. Transmitted radiance for $\mu_o = -0.1$, $\tau = 0.1$, and $A = 0$ as a function of μ. See caption for Fig. 2.

Fig. 11. Transmitted radiance for $\mu_o = -1.0$, $\tau = 1$, and $A = 0$ and 1 as a function of μ. See caption for Fig. 1.

Fig. 12. Transmitted radiance for $\mu_o = -1.0$, $\tau = 10$, and $A = 0$ and 1 as a function of μ. See caption for Fig. 1.

Fig. 13. Transmitted radiance for $\mu_o = -0.5$, $\tau = 10$, and $A = 0$ as a function of μ. See caption for Fig. 2.

Fig. 14. Transmitted radiance for $\mu_o = -0.1$, $\tau = 10$, and $A = 0$ as a function of μ. See caption for Fig. 2.

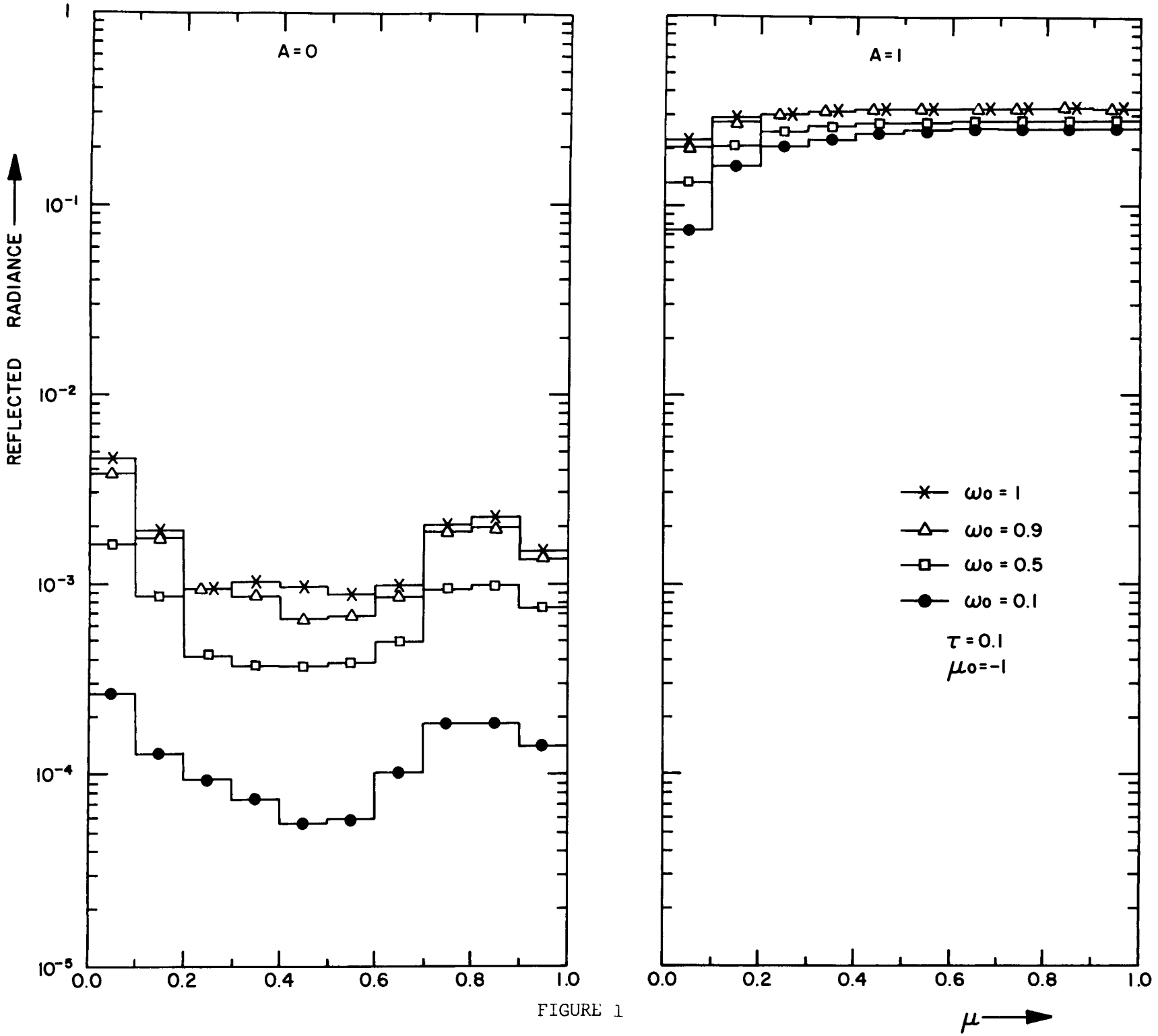
A = 0
A = 1
REFLECTED RADIANCE
1
10^{-1}
10^{-2}
10^{-3}
10^{-4}
10^{-5}
0.0
0.2
0.4
0.6
0.8
1.0
μ
$\omega_0 = 1$
$\omega_0 = 0.9$
$\omega_0 = 0.5$
$\omega_0 = 0.1$
$\tau = 0.1$
$\mu_0 = -1$

FIGURE 1

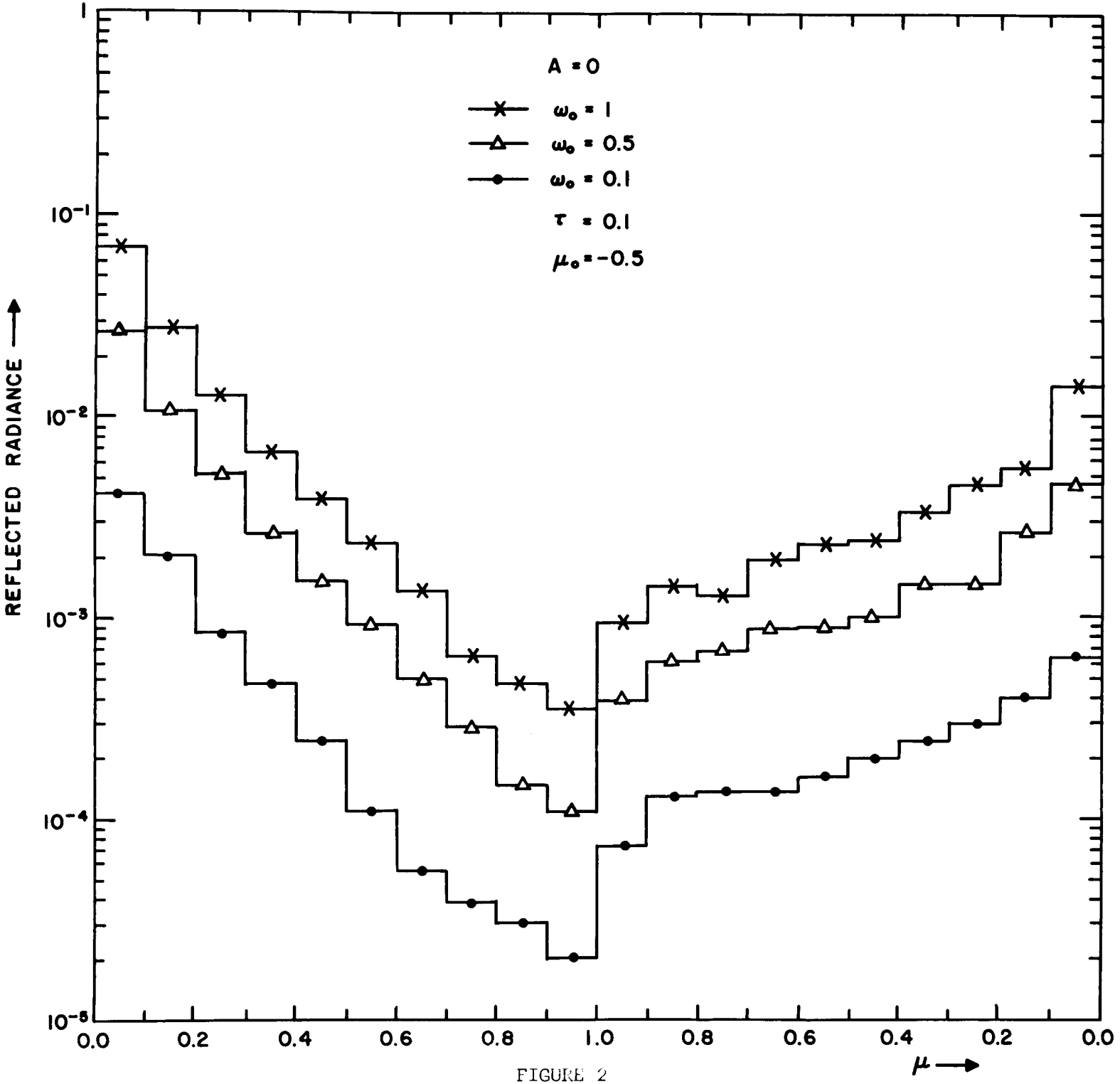
A = 0
ω_o = 1
ω_o = 0.5
ω_o = 0.1
τ = 0.1
μ_o = -0.5
REFLECTED RADIANCE
1
10^{-1}
10^{-2}
10^{-3}
10^{-4}
10^{-5}
0.0
0.2
0.4
0.6
0.8
1.0
0.8
0.6
0.4
0.2
0.0
μ

FIGURE 2

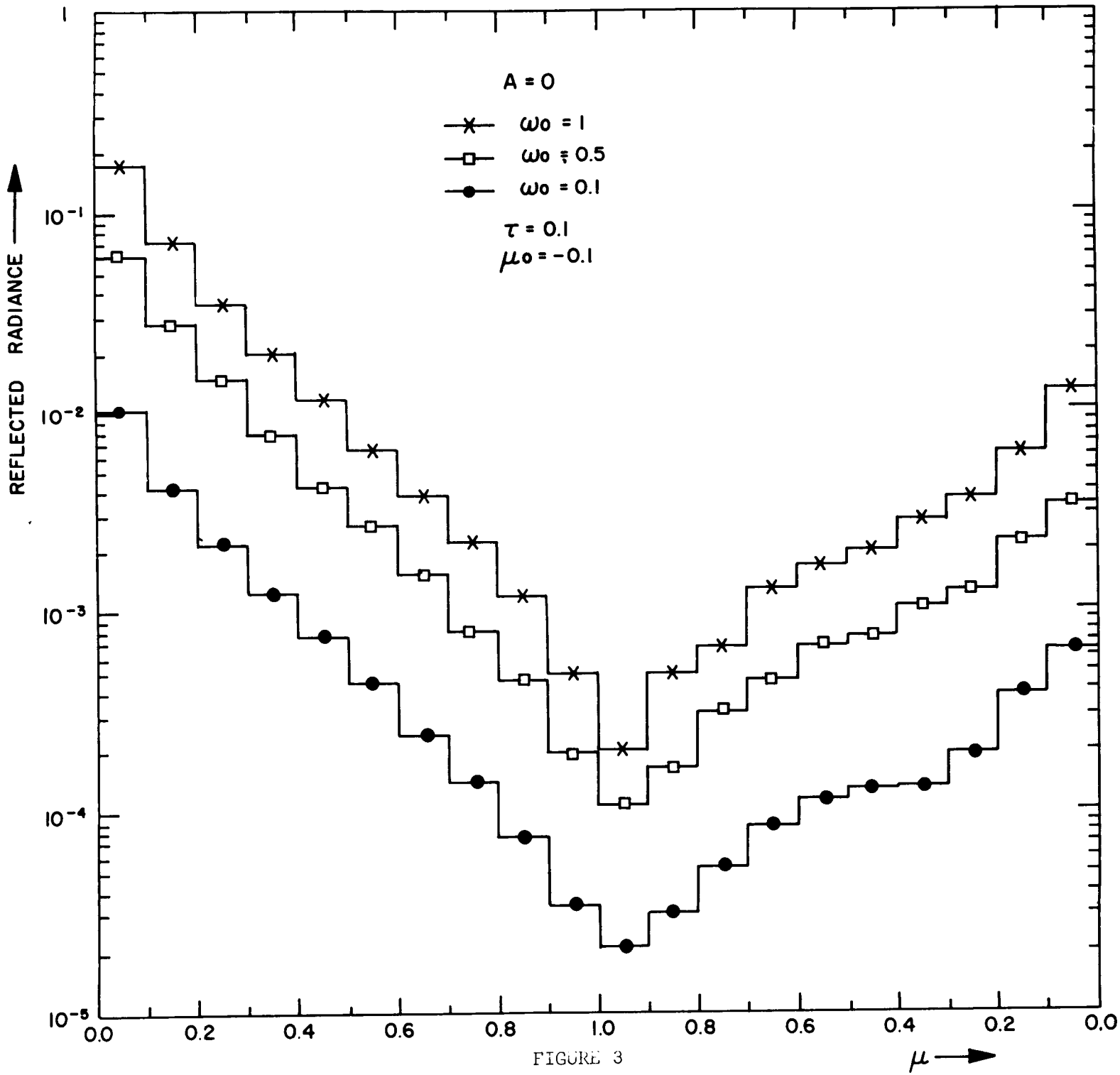
A = 0
ωo = 1
ωo = 0.5
ωo = 0.1
τ = 0.1
μo = -0.1
REFLECTED RADIANCE
1
10⁻¹
10⁻²
10⁻³
10⁻⁴
10⁻⁵
0.0
0.2
0.4
0.6
0.8
1.0
0.8
0.6
0.4
0.2
0.0
μ

FIGURE 3

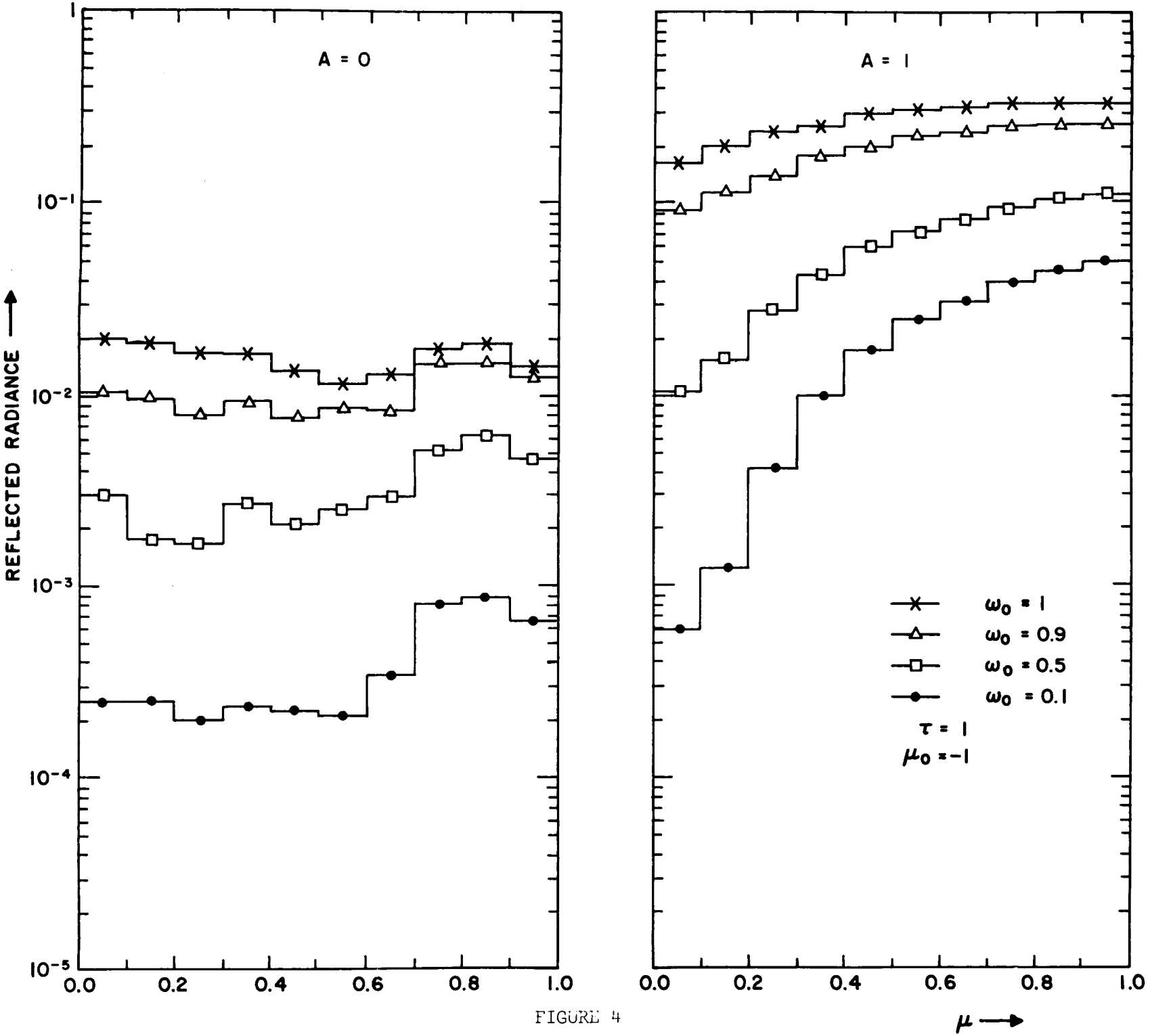
A = 0
A = 1
REFLECTED RADIANCE
1
10^{-1}
10^{-2}
10^{-3}
10^{-4}
10^{-5}
0.0
0.2
0.4
0.6
0.8
1.0
μ
ω_0 = 1
ω_0 = 0.9
ω_0 = 0.5
ω_0 = 0.1
τ = 1
μ_0 = -1

FIGURE 4

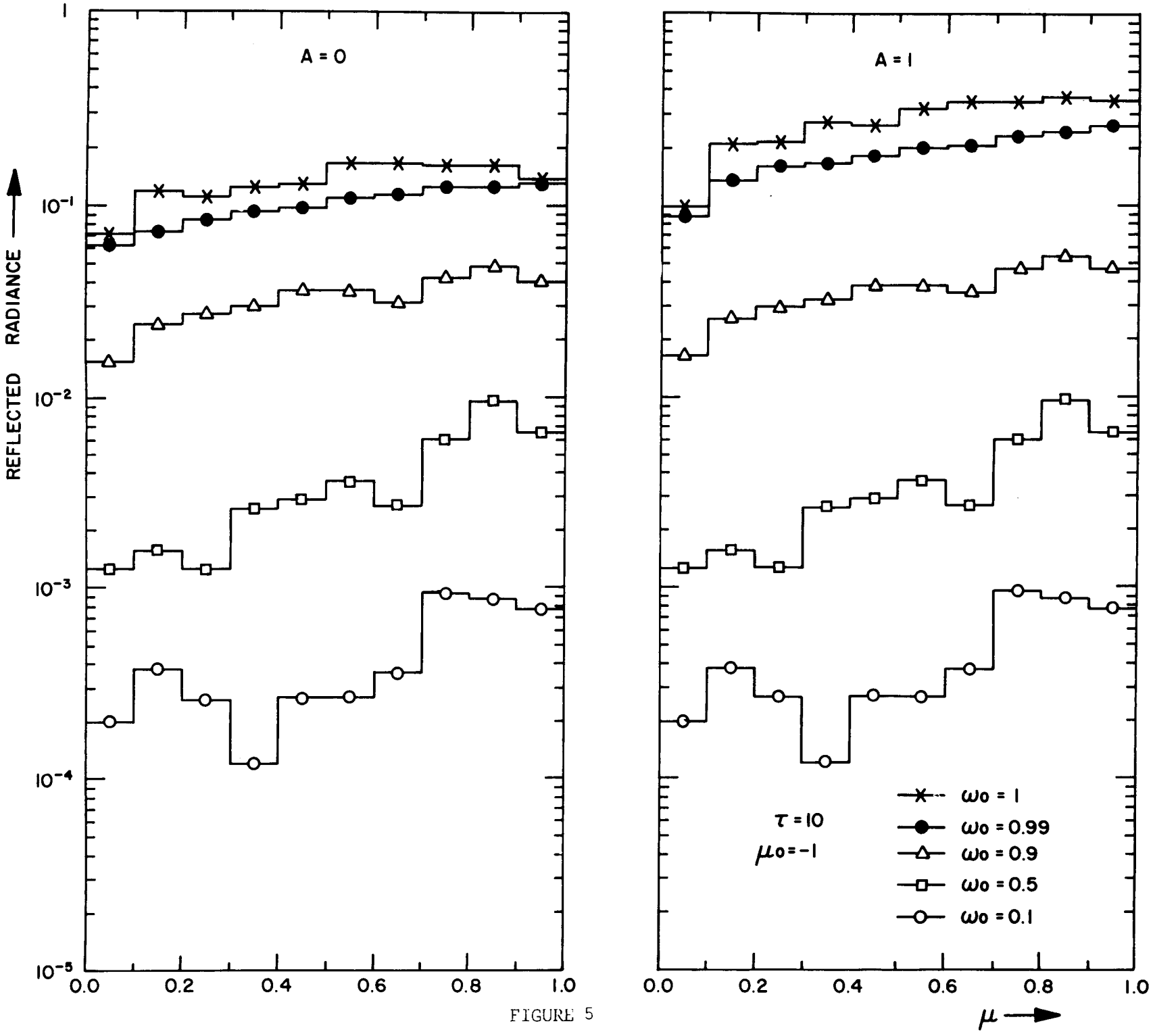
A = 0
A = 1
REFLECTED RADIANCE
1
10^{-1}
10^{-2}
10^{-3}
10^{-4}
10^{-5}
0.0
0.2
0.4
0.6
0.8
1.0
μ
$\tau = 10$
$\mu_0 = -1$
$\omega_0 = 1$
$\omega_0 = 0.99$
$\omega_0 = 0.9$
$\omega_0 = 0.5$
$\omega_0 = 0.1$

FIGURE 5

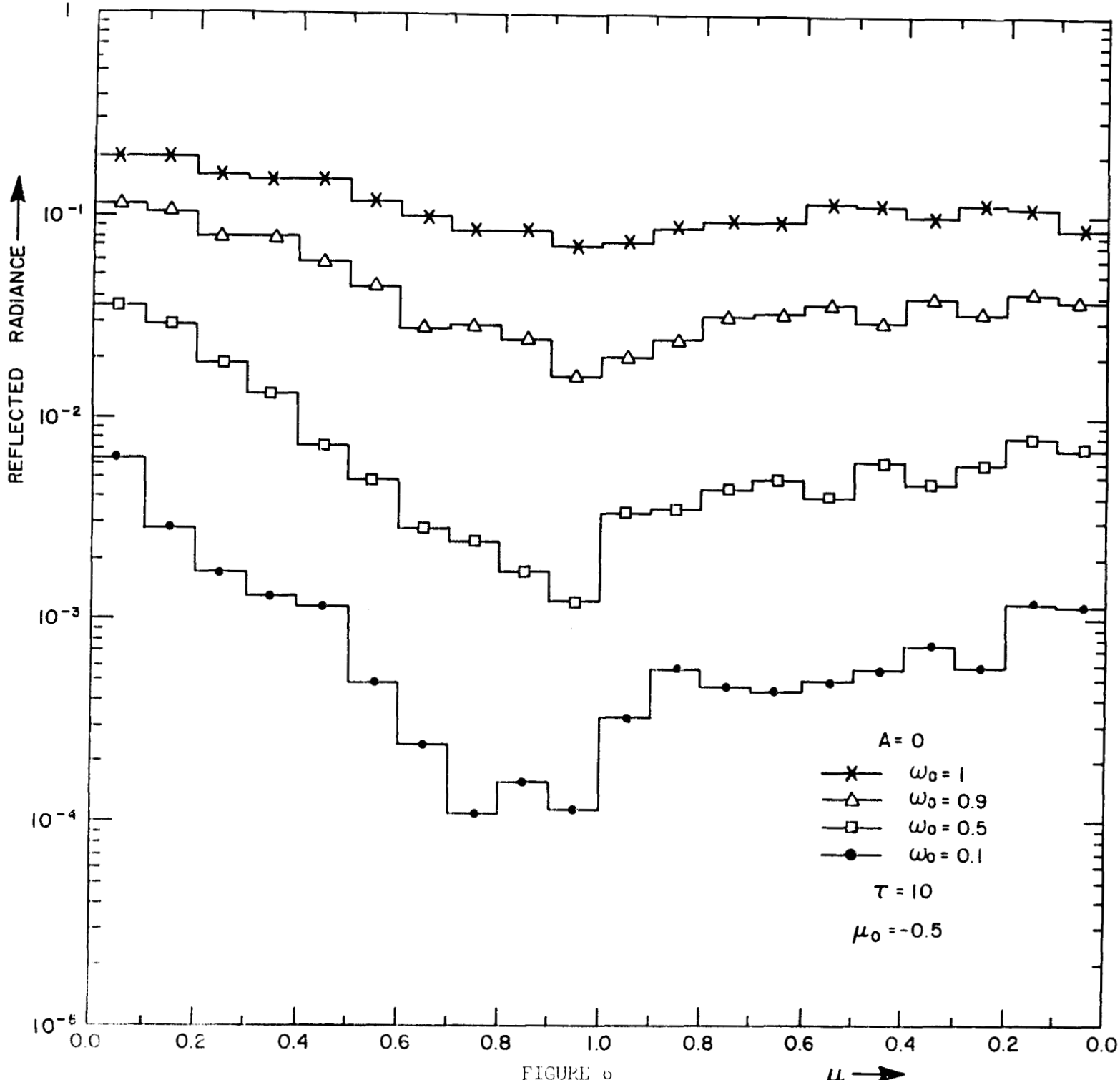
REFLECTED RADIANCE
1
10^{-1}
10^{-2}
10^{-3}
10^{-4}
10^{-5}
0.0
0.2
0.4
0.6
0.8
1.0
0.8
0.6
0.4
0.2
0.0
μ
A = 0
ω_0 = 1
ω_0 = 0.9
ω_0 = 0.5
ω_0 = 0.1
τ = 10
μ_0 = -0.5

FIGURE 6

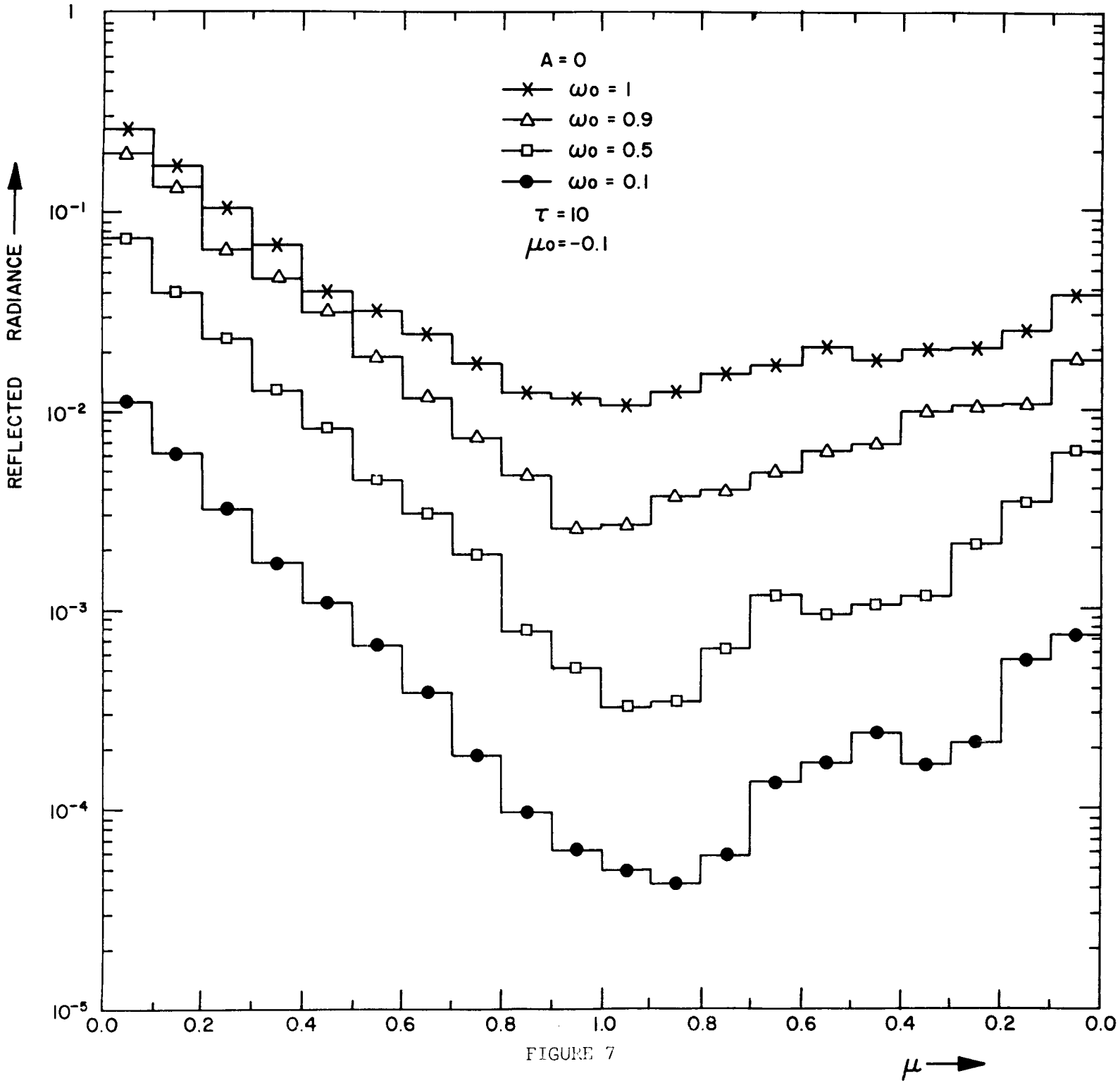
A = 0
ωo = 1
ωo = 0.9
ωo = 0.5
ωo = 0.1
τ = 10
μo = -0.1
REFLECTED RADIANCE
1
10⁻¹
10⁻²
10⁻³
10⁻⁴
10⁻⁵
0.0
0.2
0.4
0.6
0.8
1.0
0.8
0.6
0.4
0.2
0.0
μ

FIGURE 7

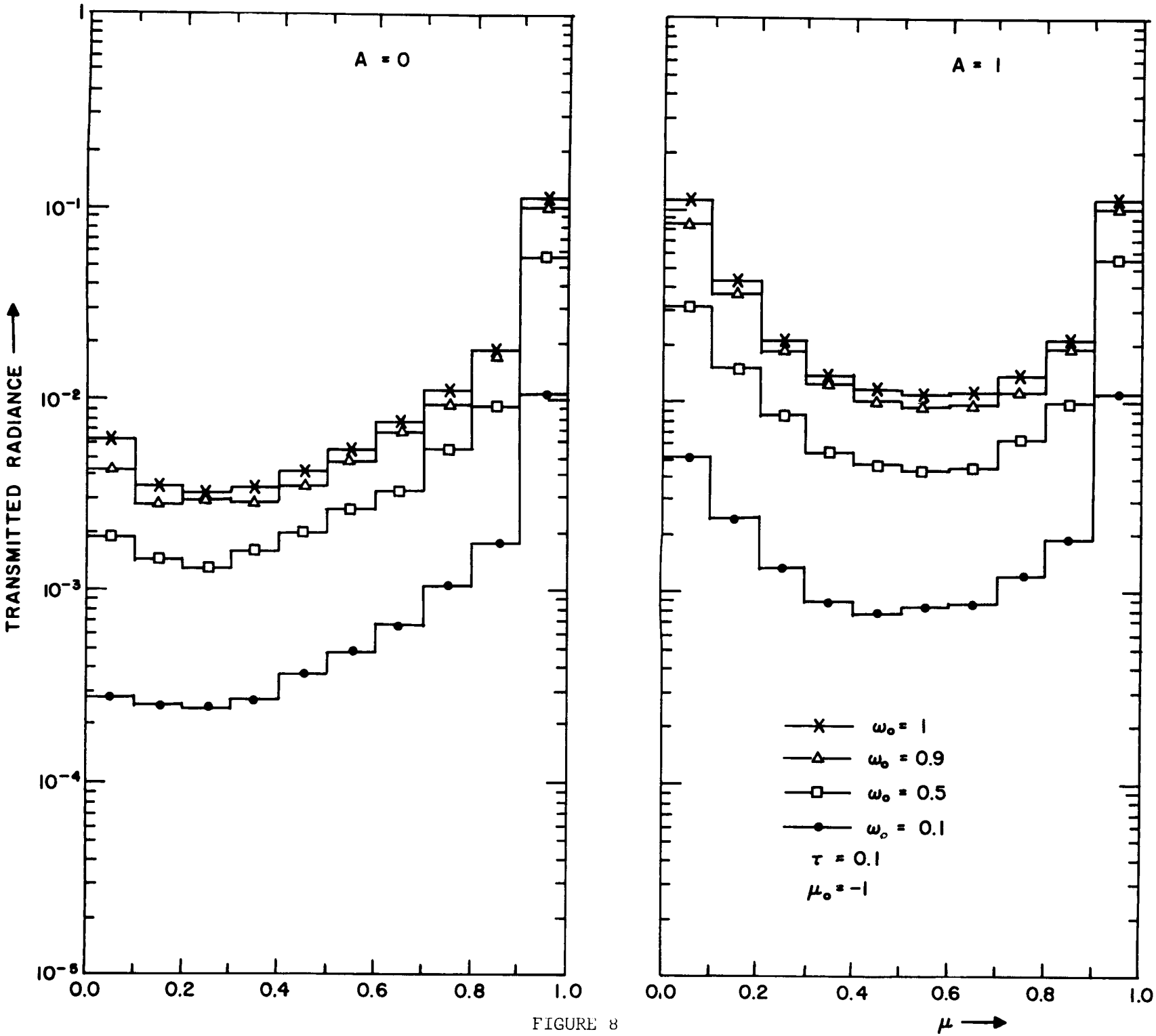
A = 0
A = 1
TRANSMITTED RADIANCE
1
10^{-1}
10^{-2}
10^{-3}
10^{-4}
10^{-5}
0.0
0.2
0.4
0.6
0.8
1.0
μ
ω_o = 1
ω_o = 0.9
ω_o = 0.5
ω_o = 0.1
τ = 0.1
μ_o = -1

FIGURE 8

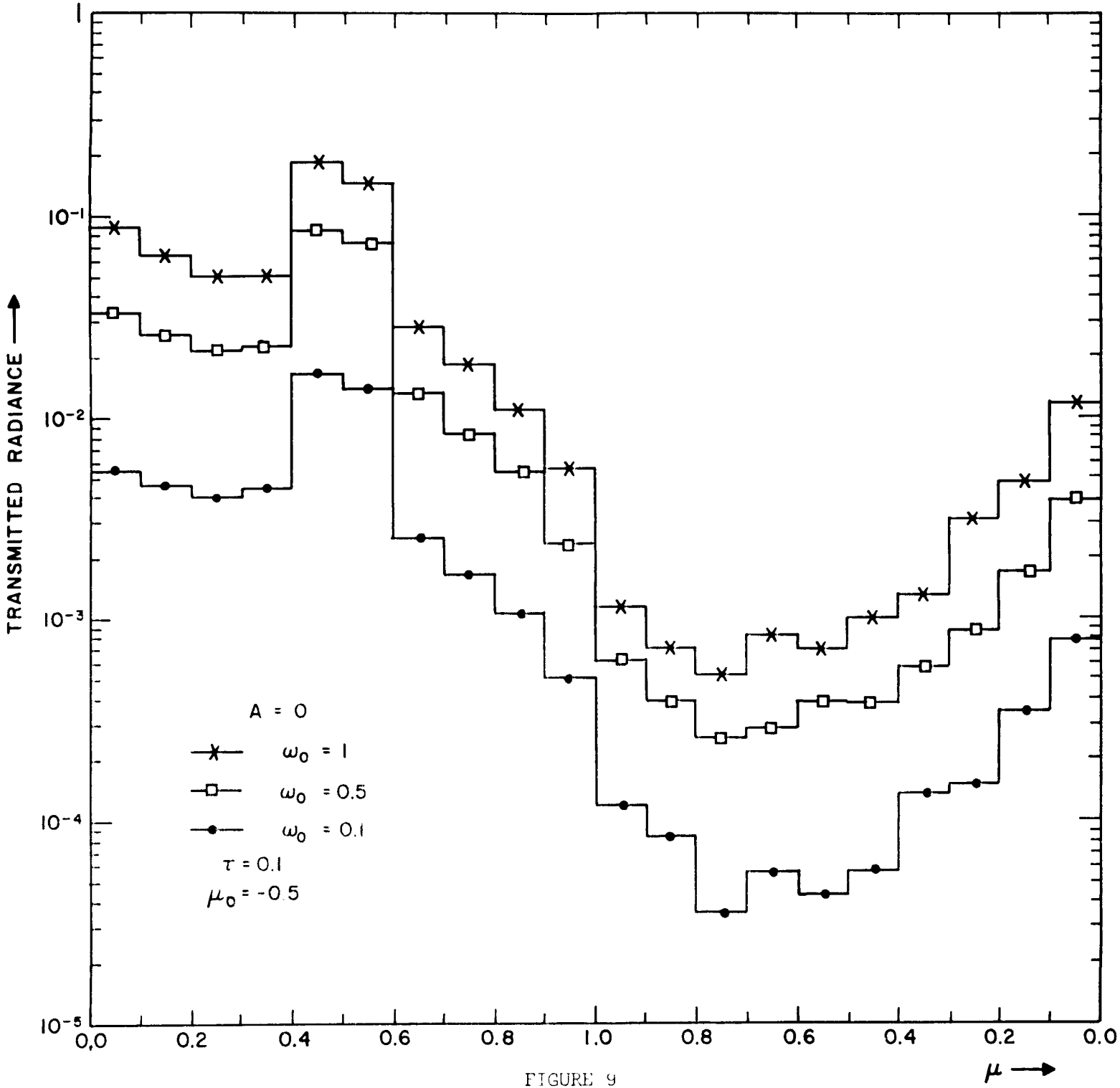
TRANSMITTED RADIANCE
1
10^{-1}
10^{-2}
10^{-3}
10^{-4}
10^{-5}
0.0
0.2
0.4
0.6
0.8
1.0
0.8
0.6
0.4
0.2
0.0
μ
A = 0
ω_0 = 1
ω_0 = 0.5
ω_0 = 0.1
τ = 0.1
μ_0 = -0.5

FIGURE 9

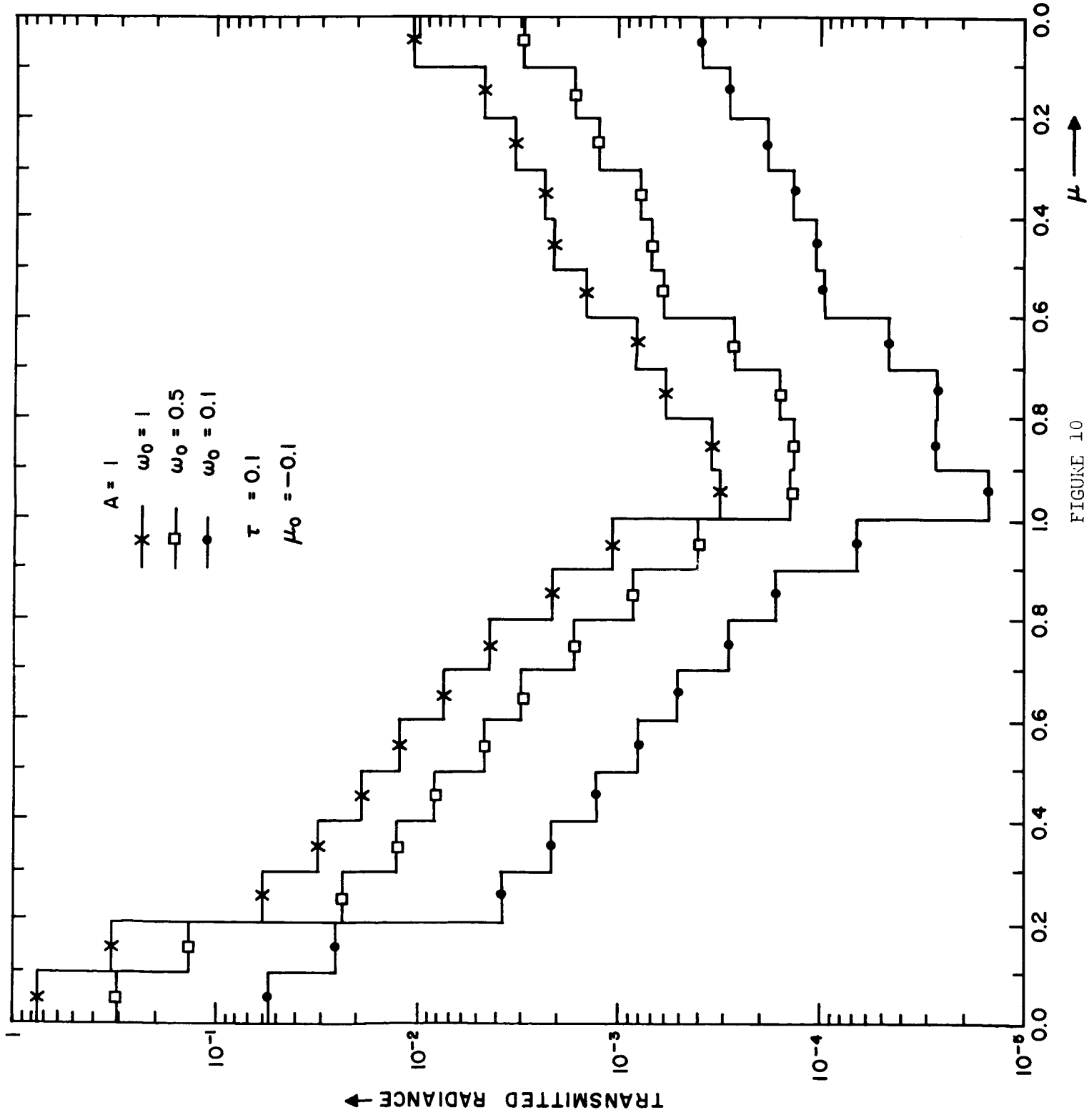
A = 1
ω₀ = 1
ω₀ = 0.5
ω₀ = 0.1
τ = 0.1
μ₀ = −0.1
TRANSMITTED RADIANCE
μ
1
10⁻¹
10⁻²
10⁻³
10⁻⁴
10⁻⁵
0.0
0.2
0.4
0.6
0.8
1.0

FIGURE 10

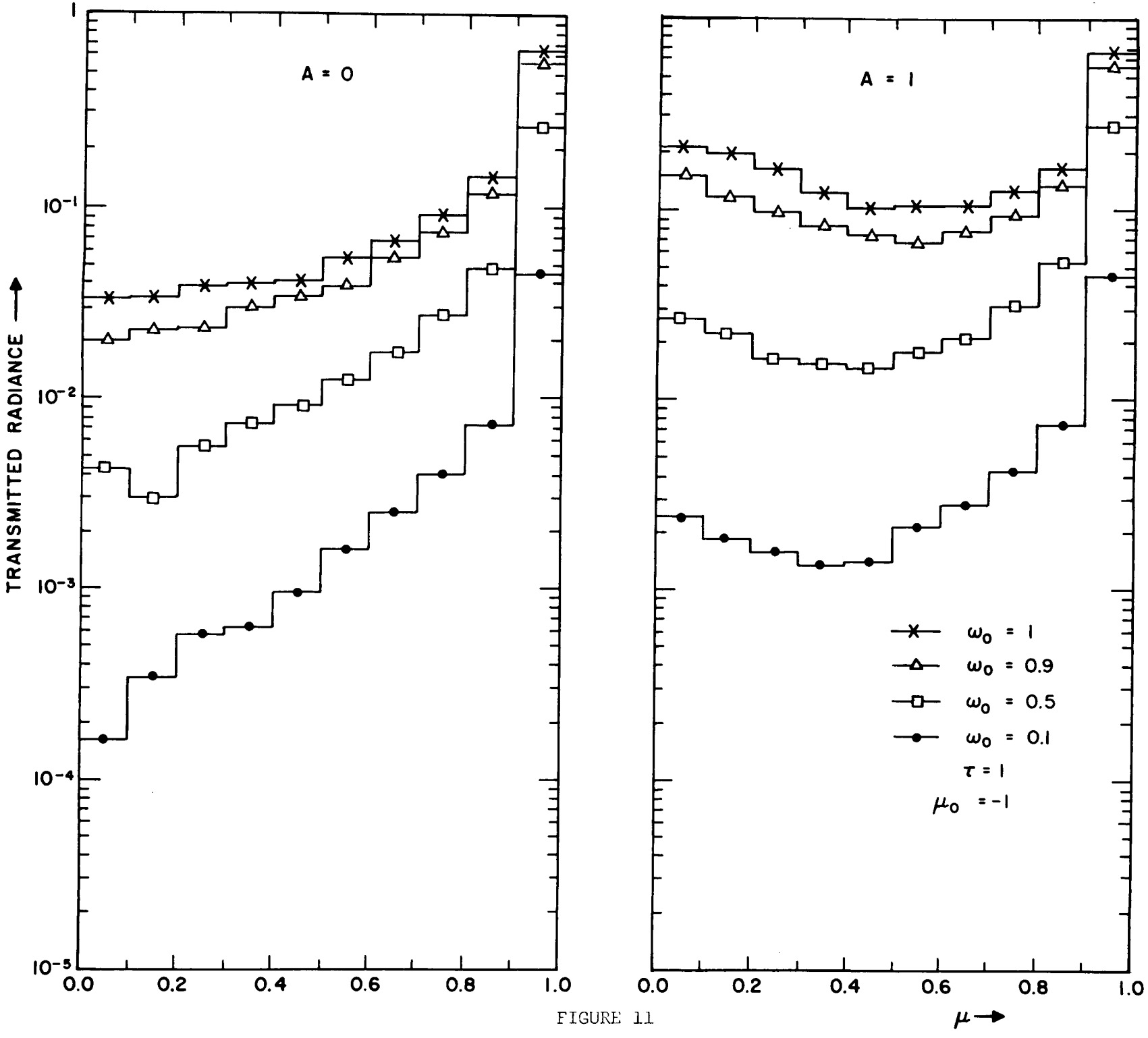
A = 0
A = 1
TRANSMITTED RADIANCE
1
10^{-1}
10^{-2}
10^{-3}
10^{-4}
10^{-5}
0.0
0.2
0.4
0.6
0.8
1.0
μ
ω_0 = 1
ω_0 = 0.9
ω_0 = 0.5
ω_0 = 0.1
τ = 1
μ_0 = -1

FIGURE 11

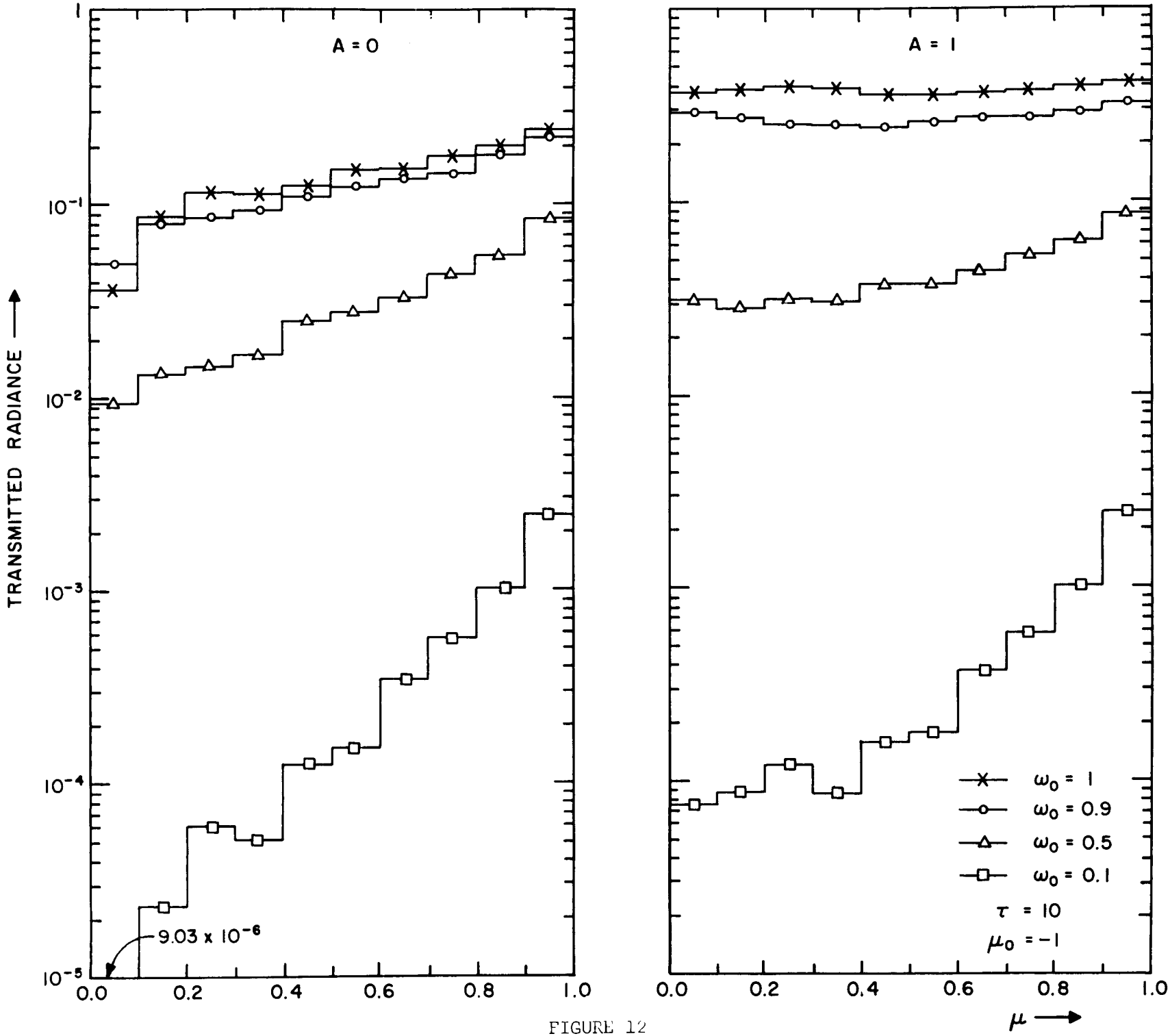
A = 0
A = 1
TRANSMITTED RADIANCE
1
10^{-1}
10^{-2}
10^{-3}
10^{-4}
10^{-5}
0.0
0.2
0.4
0.6
0.8
1.0
μ
9.03×10^{-6}
$\omega_0 = 1$
$\omega_0 = 0.9$
$\omega_0 = 0.5$
$\omega_0 = 0.1$
$\tau = 10$
$\mu_0 = -1$

FIGURE 12

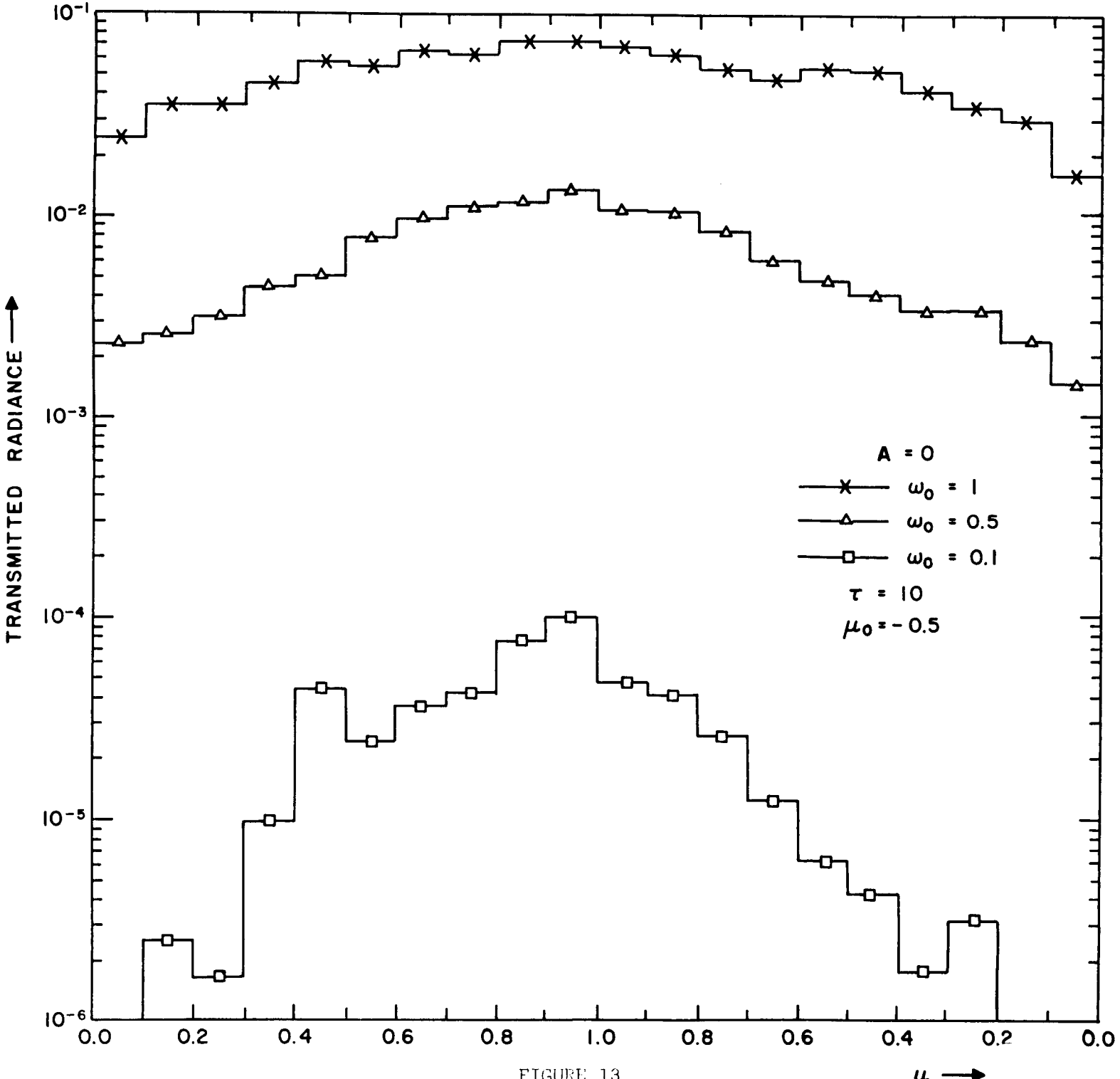
TRANSMITTED RADIANCE
10^{-1}
10^{-2}
10^{-3}
10^{-4}
10^{-5}
10^{-6}
0.0
0.2
0.4
0.6
0.8
1.0
0.8
0.6
0.4
0.2
0.0
μ
A = 0
ω_0 = 1
ω_0 = 0.5
ω_0 = 0.1
τ = 10
μ_0 = - 0.5

FIGURE 13

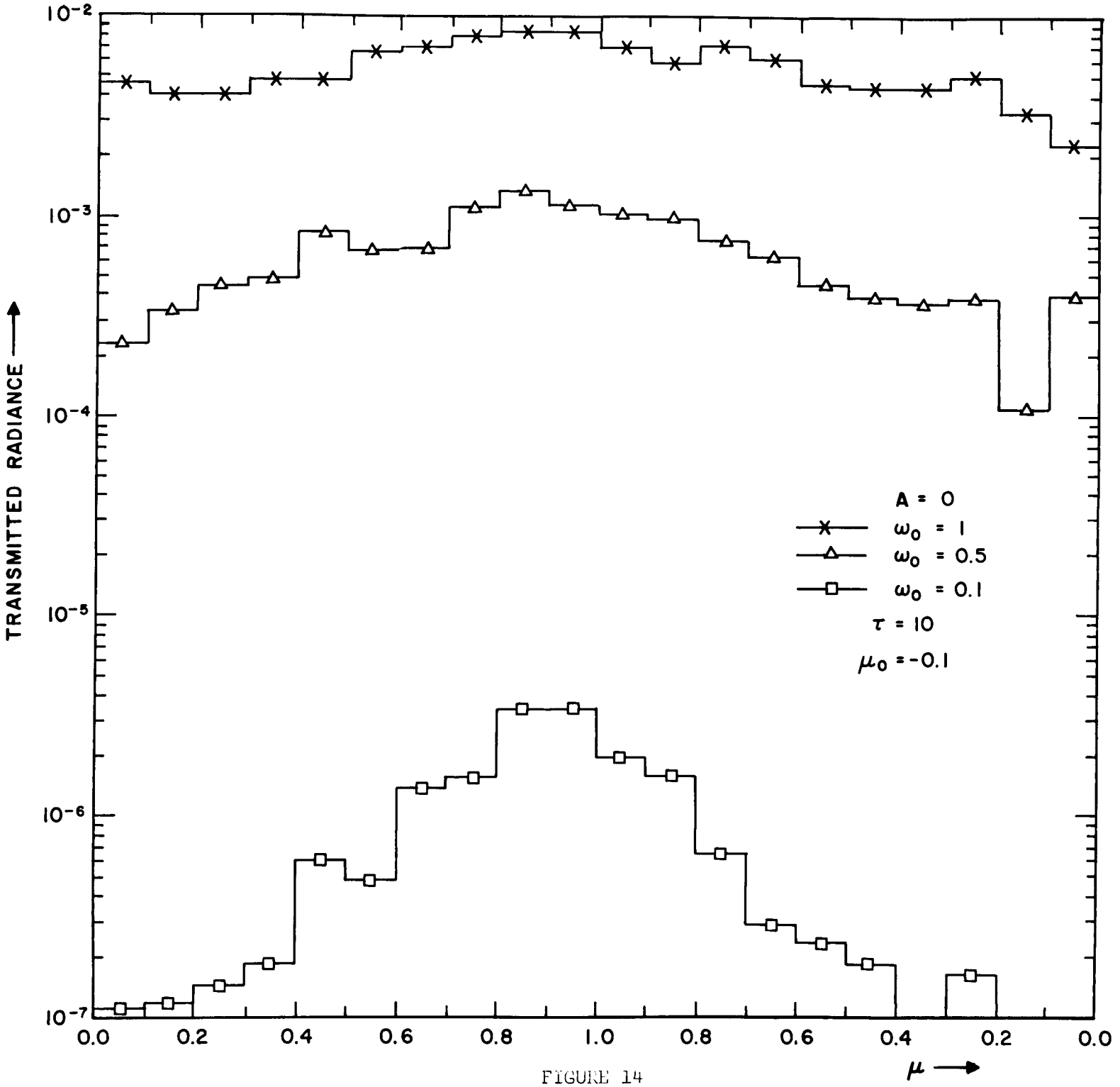
TRANSMITTED RADIANCE
10^{-2}
10^{-3}
10^{-4}
10^{-5}
10^{-6}
10^{-7}
0.0
0.2
0.4
0.6
0.8
1.0
0.8
0.6
0.4
0.2
0.0
μ
A = 0
ω_0 = 1
ω_0 = 0.5
ω_0 = 0.1
τ = 10
μ_0 = -0.1

FIGURE 14